J. Amer. Soc. Hort. Sci. 150(4):199–212. 2025. https://doi.org/10.21273/JASHS05494-25

Targeted Metabolomics-based Analysis of the Dynamics of Peel-coloration Metabolites during Purple Hawthorn Development

Kerui Jing
College of Landscape Architecture and Art, Henan Agricultural University, Zhengzhou, Henan 450002, China; and Beijing Engineering Research Center for Deciduous Fruit Trees, Key Laboratory of Biology and Genetic Improvement of Horticultural Crops (North China), Ministry of Agriculture and Rural Affairs, Institute of Forestry and Pomology, Beijing Academy of Agriculture and Forestry Sciences, Beijing 100093, China

Ningguang Dong, Jianyi Liu, Jiaqi Zuo, and Siyuan Gao
Beijing Engineering Research Center for Deciduous Fruit Trees, Key Laboratory of Biology and Genetic Improvement of Horticultural Crops (North China), Ministry of Agriculture and Rural Affairs, Institute of Forestry and Pomology, Beijing Academy of Agriculture and Forestry Sciences, Beijing 100093, China

Yonghua Li
College of Landscape Architecture and Art, Henan Agricultural University, Zhengzhou, Henan 450002, China

Jiaxin Meng
Beijing Engineering Research Center for Deciduous Fruit Trees, Key Laboratory of Biology and Genetic Improvement of Horticultural Crops (North China), Ministry of Agriculture and Rural Affairs, Institute of Forestry and Pomology, Beijing Academy of Agriculture and Forestry Sciences, Beijing 100093, China

Hongli Liu
College of Landscape Architecture and Art, Henan Agricultural University, Zhengzhou, Henan 450002, China

Keywords. anthocyanins, flavonoids, hawthorn, targeted metabolomics

Abstract. **Purple hawthorn fruit are a rare trait with considerable market and ornamental value. However, the mechanism of the accumulation of purple peel metabolites remains to be elucidated. This study used targeted metabolomics to characterize anthocyanins, carotenoids, and other flavonoids in the peel of *Crataegus pinnatifida* 'Zizhenzhu' during five developmental periods, both qualitatively and quantitatively. The analysis detected 135 metabolites in 'Zizhenzhu' peel, including 35 anthocyanins, 68 flavonoids, 24 carotenoids, six proanthocyanidins, and two chlorophylls. As fruit development progressed, the anthocyanin content increased from 20.09 $\mu g \cdot g^{-1}$ at Stage 1 (S1) to 1724.69 $\mu g \cdot g^{-1}$ at S5. A marked surge in anthocyanin content was observed at S3. Cyanidin-3-O-galactoside was identified as the predominant anthocyanin in peel, accounting for more than 92% of the total anthocyanin content. Conversely, the carotenoid content gradually declined from 202.26 $\mu g \cdot g^{-1}$ at S1 to 73.16 $\mu g \cdot g^{-1}$ at S5. Lutein was the major carotenoid, accounting for more than 70% of the total carotenoid content. Furthermore, the chlorophyll content, another pivotal substance influencing color, declined from 297.99 $\mu g \cdot g^{-1}$ at S1 to 73.68 $\mu g \cdot g^{-1}$ at S5. Phenotype and peel-coloration metabolite analysis indicated that S3 is the color-transfer period for 'Zizhenzhu' peel, and the color of hawthorn peel was ended at S5. During this process, the significant accumulation of anthocyanins and the decrease in the carotenoid and chlorophyll contents were the main reasons for the purple coloration of 'Zizhenzhu' peel at S5. This study determined the peel-coloration metabolites of 'Zizhenzhu' and their accumulation characteristics, thereby elucidating hawthorn peel coloration. Moreover, it provides a theoretical foundation for breeding to alter hawthorn peel color, as well as the development and utilization of functional components.**

Hawthorn (*Crataegus pinnatifida* 'Zizhenzhu') is a member of the Rosaceae that has many biologically active substances and nutrients, a distinct tree-like shape, and vividly colored peel (Zhang et al. 2022). Hawthorn is rich in germplasm resources, with various peel colors, including purplish-red, bright-red, and orange-red (Qin et al. 2022). Colored metabolites—such as anthocyanins, carotenoids, and chlorophylls—mainly determine plant peel color (Wang et al. 2024; Zhao et al. 2024). Furthermore, variation in the ratios of these pigments is the primary contributor to diversity in peel coloration (Muhammad et al. 2024).

Flavonoids are polyphenolic compounds such as anthocyanins, flavanols, flavonoids, flavanones, flavonols, chalcones, dihydroflavonols, and dihydrochalcones, which have a wide range of biological functions (Zhuang et al. 2023). Anthocyanins are

water-soluble secondary metabolites found widely in plant organs, including stems, leaves, flowers, and fruit, giving them blue, purple, red, and pink colors (Sharma et al. 2024). Differential anthocyanin accumulation contributes to the red and green coloration of the stem of dendrobium (*Dendrobium officinale*) (Yu et al. 2018). The anthocyanin content is significantly higher in the leaves of the purple leaf plum (*Prunus cerasifera Ehrharf*) than in the green leaves of apple (*Malus pumila var. medzwezkyena Dieck*) (Yang et al. 2024). Furthermore, there was a significant positive correlation between the color difference index and the anthocyanin content of red petals in *Rosa rugosa* (Zan et al. 2024). A significant discrepancy was observed in the anthocyanin contents of red and green Japanese apricot peel (*Prunus mume* Sieb. et Zucc.) (Ni et al. 2022). In addition to causing red–green differences, the level of anthocyanin content affects the depth of plant coloration. For example, anthocyanin content in black mulberry fruit (*Morus nigra*) is significantly higher than in red mulberry (*Morus rubra*) (Liu and Zhang 2024).

Carotenoids are natural terpenoids found in diverse plant tissues (Li et al. 2024) that confer yellow, orange, and orange-red colors depending on the different types and contents of carotenoids (Hermanns et al. 2020; Schweiggert et al. 2016; Song et al. 2024). Differential carotenoid accumulation in *Osmanthus fragrans* petals leads to yellow-white and orange-red phenotypes (Wang et al. 2018). *Lilium lancifolium* 'Splendens' petals are orange-red due to the accumulation of large amounts of capsorubin and capsanthin (Jeknic et al. 2012). Significant carotenoid accumulation results in orange mutant varieties in pink chrysanthemums (*Chrysanthemum morifolium*) (Huang et al. 2022). Carotenoids also influence fruit coloration. For instance, the orange fresh of *Malus domestica* 'Beni shogun' is attributed to the accumulation of phytoene and β-carotene, whereas *M. domestica* 'Yanfu 3' is yellow due to the accumulation of β-carotene and β-cryptoxanthin (Jia et al. 2024).

Chlorophyll plays a pivotal role in plant coloration. Different chlorophyll concentrations cause bamboo leaves to be green, green-white, or white (Zhu et al. 2024). In addition, degradation of chlorophyll also affects the coloration of citrus (*Citrus reticulata cv. Suavissima*) peel, resulting in orange or brown phenotypes (Zhu et al. 2017). The proportions of anthocyanins, carotenoids, and chlorophylls affect the color of plants (Liu et al. 2024). For example, significant differences were found in the proportions of pigments in ornamental kale leaves (*Brassica oleracea var. acephala* DC); pink leaves had the highest anthocyanin content, whereas chlorophyll and carotenoid contents were much higher in mottled pink-green leaves (Liu et al. 2021). During the development of *Euscaphis konishii* fruit, the predominant pigments in the green stage of the endocarp are chlorophyll and anthocyanins, whereas anthocyanins are the primary pigments during the red stage of the peel, with significantly higher levels than those of carotenoids and chlorophylls (Yuan et al. 2018).

There are many studies on the mechanism of fruit coloration in Rosaceae at the mature period. For example, the differential anthocyanin accumulation in the fruits of 'Xiaobai' and 'Hongyan' strawberries (*Fragaria ×ananassa*) at the mature period resulted in the distinct coloration between the varieties (Jiang et al. 2022). The differential anthocyanin accumulation caused distinct fruit coloration of 'Zhangwu', 'Nongda 5', and 'Jinou 1' (*Cerasus humilis*) at the mature period (Ji et al. 2020; Zhang et al. 2025). In red and white cherry (*Prunus tomentosa* Thunb.) fruit at the mature period, by using liquid chromatography-tandem mass spectrometry (LC-MS/MS) to analyze the flavonoid content. It was found that anthocyanins were the key coloration metabolites affecting fruit color (Zhang et al. 2022). In the 'Jinli' and 'Hujing' (*Prunus persica*) fruits, the carotenoid accumulation resulted in the differential flesh coloration (Cao et al. 2017). Many fruit color studies often investigate the mechanisms of fruit color formation by comparing the contents of key coloration metabolites of different fruit color varieties at the mature period, but other pigments except for the key coloration metabolites have been less studied during fruit development. Furthermore, many studies have investigated the metabolites involved in hawthorn peel coloration and found that the types and contents of coloration metabolites varied significantly with fruit color (Wei et al. 2025; Zhao et al. 2024). For instance, there was significant difference in anthocyanin levels of peel between red and yellow hawthorn (Çiftci et al. 2024; Zhao et al. 2022). In the same variety, various metabolite contents change significantly at different developmental stages, in 'Shandong Dajinxing' hawthorn, anthocyanins accumulate substantially at the mature period (Wang et al. 2023). Current research on hawthorn coloration metabolite focuses on hawthorn varieties with peel colors such as red and yellow. Due to the scarcity of purple hawthorn varieties, the types of coloration metabolite in fruits and the dynamic changes in the content of coloration metabolite during their development remain unclear. Therefore, this study employed targeted metabolomics to accurately quantify and classify anthocyanins, carotenoids, other flavonoids, and chlorophylls in the fruit peel of purple hawthorn 'Zizhenzhu' at five developmental stages, focusing on the types of coloration metabolite at each stage and the dynamic changes of their contents during the whole development process. We also correlated the coloration metabolite with fruit color. These results explore the color formation mechanism of purple hawthorn at the metabolite level. This study can provide a reference for the research on hawthorn fruit coloring and offer a theoretical basis for the directional genetic improvement of hawthorn fruit color as well as the development and utilization of hawthorn functional components.

Materials and Methods

Materials. This study examined 'Zizhenzhu' (*Crataegus pinnatifida*) hawthorns that showed consistent growth potential, were free of disease, and were managed in a uniform manner in the Hawthorn Germplasm Resource Nursery of the Institute of Forestry and Fruit Tree Research at Beijing Academy of Agricultural and Forestry Sciences. The trees were more than 10 years old. The experimental design examined five fruit developmental phases: S1, 70 d after bloom (DAB); S2, 90 DAB; S3, 110 DAB; S4, 130 DAB; and S5, 150 DAB (Fig. 1). Fruit

Received for publication 31 Mar 2025. Accepted for publication 20 May 2025. Published online 15 Jul 2025.
This work was supported by grants from the Research Fund for Youth of Beijing Academy of Agricultural and Forestry Science (QNJJ202409), National Natural Science Foundation of China (32401631), Beijing Academy of Agriculture and Forestry Science Innovation Capability Construction Special Project (KJCX20251401), and Youth Research Foundation of Institute of Forestry and Pomology, Beijing Academy of Agriculture and Forestry Science (LGSJJ202302).
K.J. and N.D. contributed equally to this work.
H.L. and J.M. are the corresponding authors. E-mail: liuhongli1221@henau.edu.cn and mengjiaxin@baafs.net.cn.

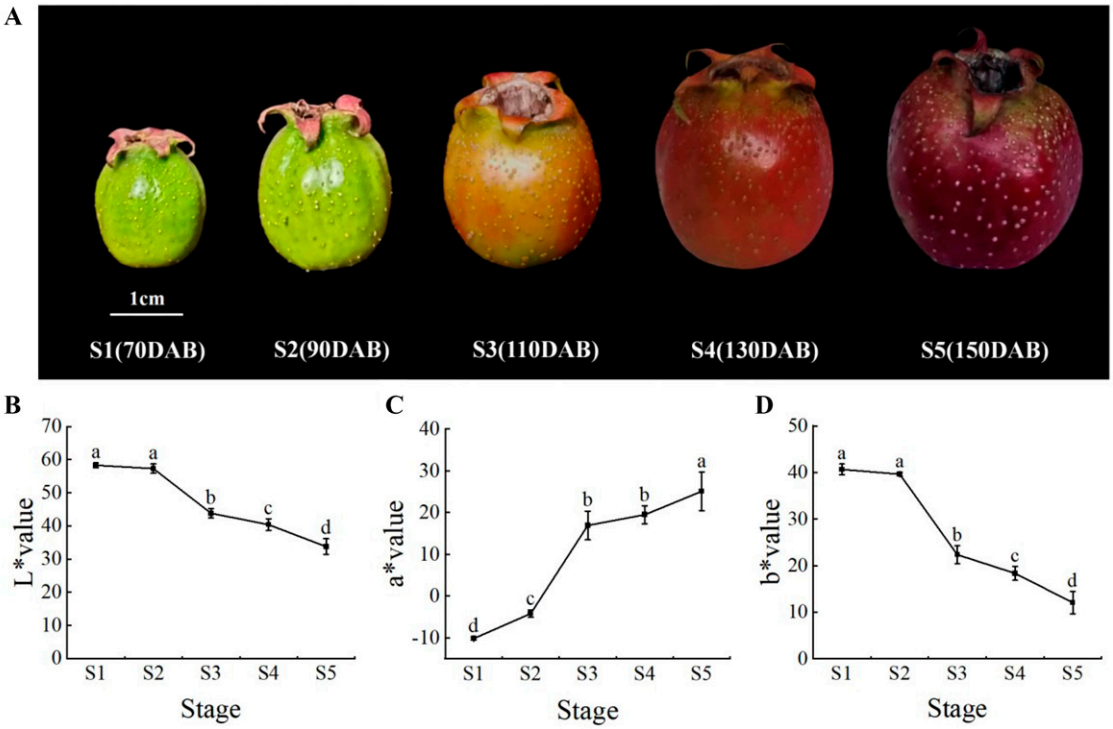

Fig. 1. Changes in peel color difference index during 'Zizhenzhu' development. (**A**) Phenotypes of 'Zizhenzhu' hawthorn fruits at the five developmental periods. (**B–D**) Changes in the L*, a*, and b* of fruit peels at the five periods in 'Zizhenzhu'. Values of five replicates are expressed as the mean ± standard deviation, and different letters indicate significant differences between groups ($P < 0.05$).

samples were collected randomly from each tree from different directions and comprised 40 healthy looking fruit of similar size per tree, and three replications per set. The hawthorn peel was promptly frozen using liquid nitrogen and stored in a refrigerator at −80 °C.

Colorimeter measurement. The peel color was determined using a colorimeter (CM-26dG, Konica Minolta, Tokyo, Japan), with measurements taken at the equatorial region of each fruit. Five fruits were randomly selected at each developmental stage, with each fruit measured five times to ensure data reliability. The colorimeter was used to measure the L*, a*, and b* values. L* values indicate lightness, with higher values corresponding to greater lightness; a* values indicate the gradation of the color from green to red, with positive values indicating red and negative values indicating green; b* values indicate the gradation of the color from blue to yellow, with positive values indicating yellowish and negative values indicating bluish.

Reagents and instruments. High performance liquid chromatography (HPLC)-grade methanol (MeOH), ethanol (EtOH), and acetonitrile (ACN) were purchased from Merck (Darmstadt, Germany), and acetone was purchased from Sinopharm (Beijing, China). Formic acid was purchased from Sigma-Aldrich (St Louis, MO, USA). Sodium chloride was from Rhawn (Shanghai, China). Potassium hydroxide was from Hushi (Shanghai, China). Methyl tert-butyl ether and n-hexane were purchased from CNW (Shanghai, China). Hydrochloric acid was obtained from Xinyang Chemical Reagent (Xinyang, China) and butylated hydroxytoluene (BHT) was purchased from Aladdin (Shanghai, China). Anthocyanin standard (50% methanol, 1 mg·mL^{-1}) was from IsoReag (Shanghai, China); the flavonoid standard (70% methanol, 10 mmol·L^{-1}) was from MCE (MedChemExpress, Shanghai, China); and the carotenoid standard (methyl tertiary butyl ether/methanol mixed solution, 1 mg·mL^{-1}) was from BOC (New York, NY, USA) and Sigma-Aldrich (St Louis, MO, USA). The QTRAP 6500 + LC-MS/MS instrument was from SCIEX (MA, Marlborough, USA); the 5424R bench-top high-speed refrigerated centrifuge was from Eppendorf (Hamburg, Germany); and the AS 60/220.R2 electronic balance was from Radwag (Radom, Poland). The MIX-200 multitube vortex oscillator was supplied by Shanghai Jingxin (Shanghai, China). The MM400 ball milling instrument was produced by Retsch (Haan, Germany). The KQ5200E ultrasonic cleaner was from Kunshan Shumei (Kunshan, China). The CentriVap centrifugal concentrator was supplied by Labconco (Kansas City, MO, USA).

Anthocyanin metabolites assay. After vacuum freeze-drying, the biological samples were ground into a powder using a ball mill at a frequency of 30 Hz. Fifty milligrams of the powdered sample was weighed and dissolved in 500 μL of 50% methanol extract (0.1% hydrochloric acid). Following dissolution of the sample, the sample extract was vortexed and ultrasonicated for 5 min. Then, the mixture was centrifuged at 4 °C and 16,904 g_n for 3 min. The resultant supernatant was aspirated and the remainder was centrifuged again. The two supernatants were combined and filtered by a membrane filter (0.22 μm, Anpel, Shanghai, China). The filtrate was collected in an injection bottle before LC-MS/MS analysis (Acevedo De la Cruz et al. 2012). The liquid-phase and mass-spectrometry conditions followed Li et al. (2022).

Flavonoid metabolite assay. The frozen samples were ground to powder using a ball mill at 30 Hz. Then, 20-mg samples were weighed and added to 500 μL of 70% methanol with 10 μL of 4000 nmol·L^{-1} internal standard solution. Following

dissolution, the sample was ultrasonicated for 30 min and centrifuged at 4 °C and at 16,904 g_n for 5 min. The upper layer was collected and filtered through a 0.22-μm microporous filter membrane. The filtrate was subsequently collected in the injection vials and used for LC-MS/MS analysis. The extraction of the flavonoids and the liquid-phase and mass-spectrometry conditions followed Shi et al. (2023).

Carotenoid metabolite assay. The frozen samples were ground to powder using a ball mill at 30 Hz. Then, 50-mg samples were dissolved in 500 μL of a mixture of hexane, acetone, and ethanol (1:1:1 v/v/v), containing 0.01% BHT ($g \cdot mL^{-1}$), and vortexed for 20 min. The extract sample was then centrifuged for 5 min at 4 °C and 16,904 g_n. The upper layer was aspirated and the above process was repeated for the remainder. The two supernatants were combined and concentrated. Then, they were reconstituted in 100 μL of a 1:1 methanol/methyl tertiary butyl ether mixture solution (v/v), filtered through a 0.22-μm microporous filter membrane, and the filtrate was collected in brown injection vials for LC-MS/MS analysis (Amorim-Carrilho et al. 2014). The liquid-phase and mass-spectrometry conditions followed the methods of Krinsky et al. (2004) and Geyer et al. (2004).

Chlorophyll metabolite assay. Approximately 0.1 g of hawthorn peel was weighed and ground into powder in liquid nitrogen. Then, the powder was immersed in 10 mL of 95% ethanol solution for 12 h in the dark at room temperature. Next, the mixture was centrifuged at 16,904 g_n for 10 min. The resultant pellet was then removed, and the remaining liquid was collected. The chlorophyll concentration was then determined by measuring the light-absorption values of the extract at 665 nm (D_{665}) and 649 nm (D_{649}) (Dai et al. 2024). The following formulas were used for calculating the chlorophyll content:

$$\text{Chl a} = (13.95 \times D_{665} - 6.88 \times D_{649}) \times V/1000\,M$$
$$\text{Chl b} = (24.96 \times D_{649} - 7.32 \times D_{665}) \times V/1000\,M,$$
$$\text{Total Chl} = \text{Chl a} + \text{Chl b}$$

where Chl a is the chlorophyll a concentration ($mg \cdot g^{-1}$), Chl b is the chlorophyll b concentration ($mg \cdot g^{-1}$), V is the total volume of extract (mL), and M is the sample mass (g).

Data analysis. The data were characterized and quantified using a custom Wuhan Mavis Metabolism Biotechnology (MWDB, Wuhan, China) database combined with the multiple reaction monitoring mode of triple quadrupole mass spectrometry. The mass spectrometry data were collected and analyzed by R software and Origin2022 software. Data represent the mean ± standard deviation from at least three experiments. Statistical significance was defined as $P < 0.05$.

Results

Comparison of color changes during hawthorn fruit development. The color of the 'Zizhenzhu' peel gradually changed from green to purple as the fruit developed (Fig. 1A). During development, the L* value decreased continuously, to a value of 33.79 at S5 (Fig. 1B); the a* value increased continuously, becoming positive at S3 with a value of 16.92, and reached a maximum value of 25.09 at S5 (Fig. 1C). Conversely, the b* value decreased continuously, from 40.65 at S1 to 12.04 at S5, corresponding to the phenotype change of the peel from green to purple (Fig. 1D). S3 was the critical period for color change in 'Zizhenzhu', when the peel transitioned from green to red. S4 and S5 corresponded to the mid- and late-coloring stages of fruit color development, respectively.

Comparison of peel metabolites during fruit development. A total of 135 metabolites were identified in 'Zizhenzhu' peel, including 35 anthocyanins, 24 carotenoids, 21 flavones, 21 flavanols, six proanthocyanidins, six flavanols, five flavanones, four flavanonols, four chalcones, four flavone glycosides, three isoflavanones, chlorophyll a, and chlorophyll b (Table 1). Detailed metabolite information is provided in Supplemental Table 1.

During the five developmental periods, 92 metabolites were detected in 'Zizhenzhu' peel, with three, two, and nine metabolites specific to S1, S4, and S5, respectively (Fig. 2A). Principal component analysis (PCA) was used to compare the metabolite composition of 'Zizhenzhu' peel in the five different developmental periods (Fig. 2B). The quality control samples (mix) were projected to the same region in the PCA plot. Moreover, the three biological replicates from each different period were clustered in the same region, indicating that the replicates shared very similar metabolic profiles, ensuring the reliability and reproducibility of the results. The metabolites from the five periods tended to differentiate along the first (PC1) and second principal component (PC2). Metabolites from adjacent developmental periods segregated about equally on PC1, whereas two periods (S1 and S5) were significantly segregated from S2, S3, and S4 on PC2. These results indicate that the metabolites in 'Zizhenzhu' hawthorn peels vary significantly across different developmental periods. Periods S1 and S5 differed the most markedly on PC1, implying that the metabolites present in S1 and S5 differ considerably. These divergent metabolites may play a crucial role in the change in peel color from green to purple.

Analysis of anthocyanin and proanthocyanidin metabolites in peel during fruit development. A total of 35 anthocyanins were detected and their abundance varied significantly among samples (Fig. 3A). The total anthocyanin content of the peel increased continuously with fruit development. There were fewer anthocyanins at S1 and S2, which were 20.09 $\mu g \cdot g^{-1}$ and 75.70 $\mu g \cdot g^{-1}$, respectively. Subsequently, significant anthocyanin accumulation occurred, reaching 384.85 $\mu g \cdot g^{-1}$ at S3 and 1479.26 $\mu g \cdot g^{-1}$ at S4. Finally, anthocyanin accumulated to a maximum value of 1724.69 $\mu g \cdot g^{-1}$ at S5 (Fig. 3B). To identify anthocyanin differential metabolites in the 'Zizhenzhu' peel during development, their contents at different stages were compared. Comparing S1 vs. S2, S2 vs. S3, S3 vs. S4, and S4 vs. S5, there were 16, 11, 14, and 7 upregulated anthocyanin

Table 1. Qualitative and quantitative results of metabolites in fruit peels of *Crataegus pinnatifida* 'Zizhenzhu'.

Ranking	Metabolite categories	Number
1	Anthocyanins	35
2	Carotenoids	24
3	Flavones	21
4	Flavonols	21
5	Proanthocyanidins	6
6	Flavanols	6
7	Flavanones	5
8	Flavone glycosides	4
9	Flavanonols	4
10	Chalcones	4
11	Isoflavanones	3
12	Chlorophyll	2

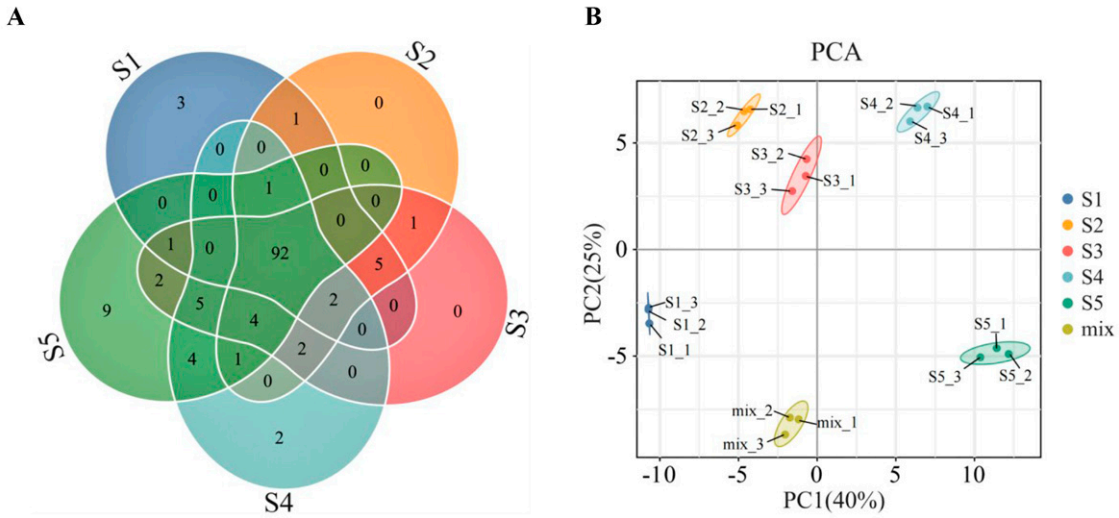

Fig. 2. Comparison of metabolites and principal component analysis during development of 'Zizhenzhu'. (**A**) Comparison of metabolites at the five periods in 'Zizhenzhu'. (**B**) Principal component analysis (PCA) of peel metabolites at the five periods in 'Zizhenzhu'.

metabolites, respectively, and 2, 2, 4, and 7 downregulated anthocyanin metabolites (Fig. 3C). Bar graphs of the differential metabolites were plotted by comparing the multiplicity of differences resulting from quantitative information on anthocyanin metabolites at different times. In the comparison between S1 and S2, this showed that derivatives of cyanidin, petunidin, and delphinidin were significantly upregulated (Fig. 3D). Comparing S2 and S3, the derivatives of cyanidin, petunidin and peonidin were significantly upregulated, whereas some derivatives of petunidin were significantly downregulated (Fig. 3E). In the comparison between S3 and S4, the derivatives of cyanidin, peonidin, delphinidin, pelargonidin, and petunidin were significantly upregulated (Fig. 3F). Comparing S4 and S5, some pelargonidin and cyanidin derivatives were significantly upregulated, and some derivatives of delphinidin, pelargonidin, and cyanidin were significantly downregulated (Fig. 3G). In these four comparisons, the significantly upregulated anthocyanin metabolites were primarily cyanidin derivatives, while the significantly downregulated anthocyanin metabolites were primarily pelargonidin and delphinidin derivatives. Specifically, cyanidin-3-O-galactoside accumulated significantly during 'Zizhenzhu' development, accounting for more than 92% of the total anthocyanin content throughout the development process, its content reaching a maximum value (1606.60 $\mu g \cdot g^{-1}$) at S5 (Fig. 3H). Furthermore, cyanidin-3-O-arabinoside and peonidin-3-O-arabinoside accumulated continuously, reaching maximum values of 53.60 $\mu g \cdot g^{-1}$ (Fig. 3I) and 46.71 $\mu g \cdot g^{-1}$ (Fig. 3J), respectively, at S5.

In summary, the change in the cyanidin-3-O-galactoside content was the main factor leading to the change in the total anthocyanin content, especially at S3, when its accumulation (356.23 $\mu g \cdot g^{-1}$) was the main reason for the change in color of 'Zizhenzhu' peel from green to red.

The proanthocyanidin content showed a "single peak" tendency, reaching a maximum value of 7659.69 $\mu g \cdot g^{-1}$ at S4, and declining to 7328.69 $\mu g \cdot g^{-1}$ at S5. The proanthocyanidin content changed smoothly from one period to the next (Fig. 4A). Procyanidin B2 was the predominant proanthocyanidin in the 'Zizhenzhu' peel, accounting for 87.86% of the total proanthocyanidin content, followed by procyanidin C1 (11.78%) at S5 (Fig. 4B).

Analysis of other flavonoid metabolites in peel during fruit development. The abundance of 68 flavonoid compounds other than anthocyanins and proanthocyanidins in peel varied significantly among samples (Fig. 5A). The total content of these 68 flavonoids showed a "bimodal" trend, with rapid increase to 4250.97 $\mu g \cdot g^{-1}$ at S2 and 4621.36 $\mu g \cdot g^{-1}$ at S4, and a decrease to 4256.63 $\mu g \cdot g^{-1}$ at S5 (Fig. 5B). Comparing these flavonoids in 'Zizhenzhu' peel during S1 vs. S2, S2 vs. S3, S3 vs. S4, and S4 vs. S5, 19, 6, 7, and 11 flavonoid metabolites were upregulated, respectively, and 2, 5, 3, and 5 were downregulated (Fig. 5C). Bar graphs of the differential metabolites were plotted by comparing the multiplicity of differences resulting from quantitative information on these flavonoid metabolites at different times. Between S1 and S2, flavonols, flavones, flavone glycosides, and chalcones were significantly upregrated (Fig. 5D). Comparing S2 and S3, flavones, flavonols, and flavanols were significant upregulated, while flavone glycosides and other flavones were significant downregulated (Fig. 5E). Comparing S3 and S4, flavanols and flavones were significantly upregulated (Fig. 5F). Comparing S4 and S5, flavonols, flavones, and some flavanones were significantly upregulated, while flavone glycosides and other flavanols were significantly downregulated (Fig. 5G). Overall, in these four sets of comparisons, the significantly upregulated flavonoid metabolites were mainly flavonols, flavones, and flavanols, while the significantly downregulated flavonoid metabolites were mainly flavone glycosides.

To analyze the changes in these flavonoid contents, five flavonoids that accounted for ≈92% of the total content of 68 flavonoids were selected. As shown in Fig. 5H, (–)-epicatechin, which accounted for more than 56% of the total content of these flavonoids throughout the development, showed a "bimodal" trend, with the content reaching 2877.15 $\mu g \cdot g^{-1}$ at S1, decreasing to a minimum of 2389.97 $\mu g \cdot g^{-1}$ at S3, increasing to 2753.61 $\mu g \cdot g^{-1}$ at S4, and falling to 2660.93 $\mu g \cdot g^{-1}$ at S5 (Fig. 5H). Hyperoside content increased from a minimum value of 298.10 $\mu g \cdot g^{-1}$ at S1 to a maximum of 651.46 $\mu g \cdot g^{-1}$ at S3, and then decreasing slightly to 604.09 $\mu g \cdot g^{-1}$ at S5 (Fig. 5I).

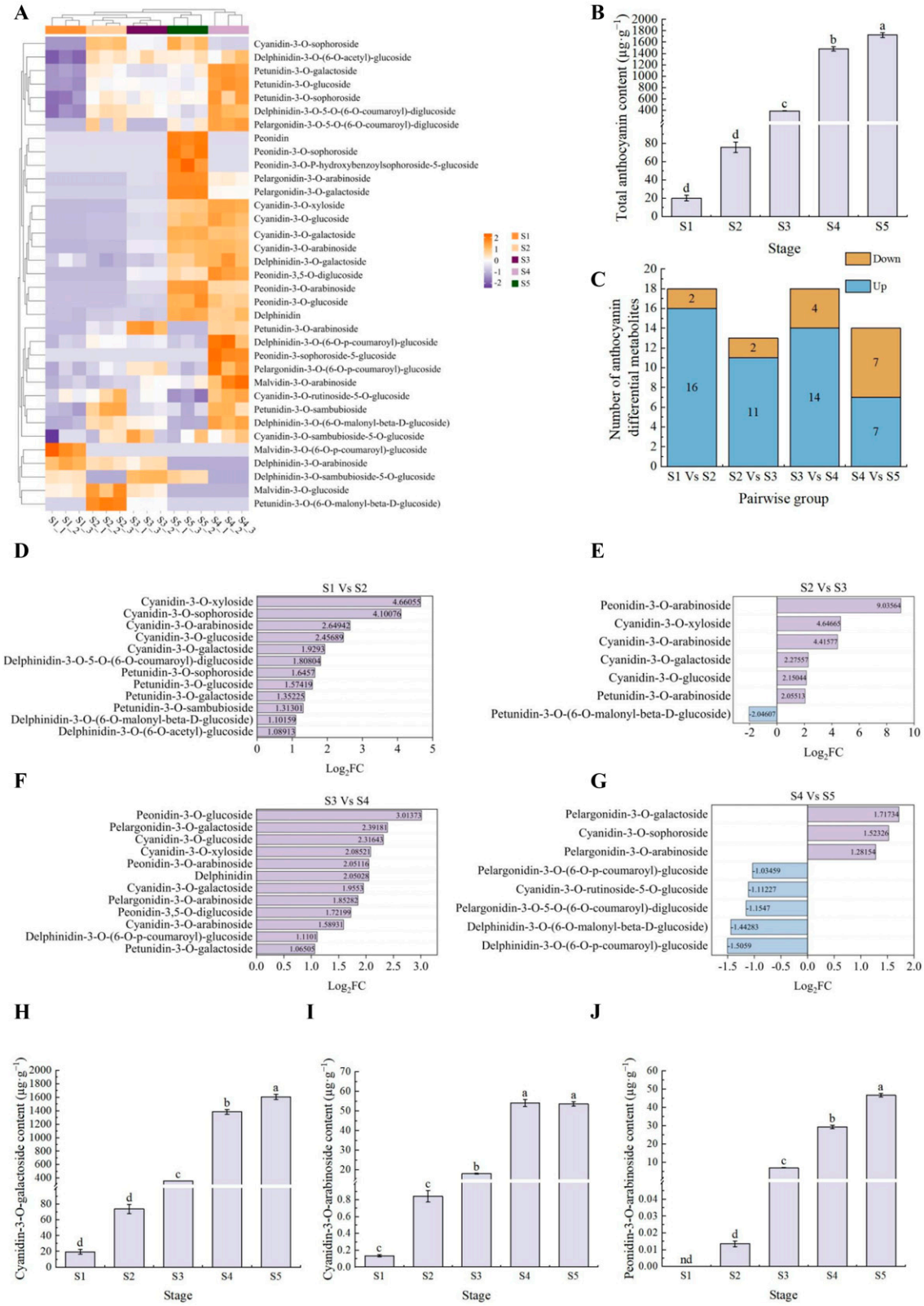

Fig. 3. Analysis of anthocyanin metabolites in the peel during 'Zizhenzhu' fruit development. (**A**) Heatmap of anthocyanin metabolites clustering in the peel of 'Zizhenzhu' during fruit development. Each column in the heatmap represents a sample and each row represents a metabolite. Different colors in the heatmap represent different metabolite contents. Yellow and purple colors indicate higher or lower metabolite levels, respectively. (**B**) Changes in the content of total anthocyanins in the 'Zizhenzhu' peel. (**C**) The number of upregulated and downregulated differential anthocyanin metabolites in the 'Zizhenzhu' peel. (**D–G**) Histograms of the differential multiplicity of anthocyanin differential metabolites in the 'Zizhenzhu' peel ($Log_2FC \neq \pm$ Inf). (**H**) Changes in the content of cyanidin-3-O-galactoside in the 'Zizhenzhu' peel. (**I**) Changes in the content of cyanidin-3-O-arabinoside in the 'Zizhenzhu' peel. (**J**) Changes in the content of peonidin-3-O-arabinoside in the 'Zizhenzhu' peel. Values of three replicates are expressed as the mean ± standard deviation. Different letters indicate significant differences between groups ($P < 0.05$), and nd (not found) indicates that no substance content was detected.

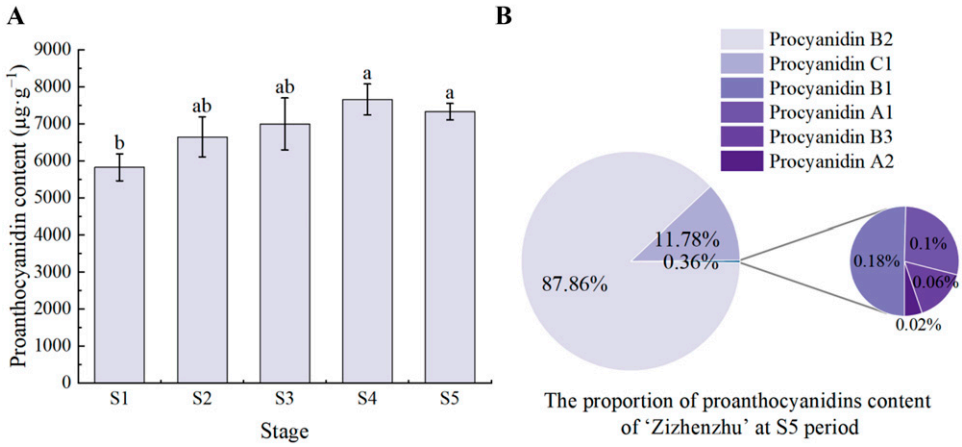

Fig. 4. Analysis of proanthocyanidin metabolites in the peel during 'Zizhenzhu' fruit development. (**A**) Changes in the content of total proanthocyanidins in the 'Zizhenzhu' peel. (**B**) Proanthocyanidin components content percentage in 'Zizhenzhu' at S5. Values of three replicates are expressed as the mean ± standard deviation and different letters indicate significant differences between groups ($P < 0.05$).

Quercetin-3-O-glucoside also showed a "bimodal" trend, increasing to 334.49 μg·g^{-1} at S2 and 441.23 μg·g^{-1} at S4, and decreasing to 207.43 μg·g^{-1} at S5 (Fig. 5J). Baimaside showed a "single peak" trend, reaching minimum and maximum values of 37.82 μg·g^{-1} and 297.58 μg·g^{-1} at S1 and S3, respectively, and 224.66 μg·g^{-1} at S5 (Fig. 5K). Rutin showed a "single peak" trend, with the minimal value of 187.24 μg·g^{-1} at S1, and rapidly increasing to a maximum value of 261.89 μg·g^{-1} at S2 and then decreasing to 186.55 μg·g^{-1} at S5 (Fig. 5L).

Of the five major flavonoids—(–)-epicatechin, hyperoside, quercetin-3-O-glucoside, baimaside, and rutin—(–)-epicatechin does not affect color, whereas the levels of the four metabolites (hyperoside, quercetin-3-O-glucoside, baimaside, and rutin) did not vary markedly between adjacent developmental periods, implying that these metabolites are not the primary drivers of the changes observed in fruit coloration.

Analysis of carotenoid metabolites in peel during fruit development. A total of 24 carotenoids were detected and their abundance varied significantly among the different samples (Fig. 6A). The total carotenoid content of the peel decreased gradually from a maximum value of 202.26 μg·g^{-1} at S1 to a minimum value of 73.16 μg·g^{-1} at S5 (Fig. 6B). Comparing carotenoids in 'Zizhenzhu' peel during S1 vs. S2, S2 vs. S3, S3 vs. S4, and S4 vs. S5, the results showed that two, zero, three, and eight carotenoid metabolites were upregulated and one, two, three, and three carotenoid metabolites were downregulated, respectively (Fig. 6C). Bar graphs of the differential metabolites were plotted by comparing the multiplicity of differences resulting from quantitative information on carotenoid metabolites at different times. The comparison between S1 and S2, zeaxanthin and (E/Z)-phytoene were significantly upregulated, whereas α-carotene was significantly downregulated (Fig. 6D). Between S2 and S3, α-carotene was significantly downregulated (Fig. 6E). Between S3 and S4, lutein dilaurate was significantly upregulated and violaxanthin was significantly downregulated (Fig. 6F). Between S4 and S5, violaxanthin dioleate, neochrome palmitate, lutein dimyristate, lutein dilaurate, and lutein palmitate were significantly upregulated and α-carotene was significantly downregulated (Fig. 6G). The contents of these divergent metabolites fluctuated within 0% to 6.34% (Fig. 7A). Despite the substantial variation in the contents over the course of development, they were not deemed significant contributors to the changes in total carotenoid content, due to their minimal levels.

Therefore, we selected 12 carotenoids that accounted for ∼99% of the total carotenoid content for detailed analysis (Fig. 7B). Among these, lutein accounted for more than 70% of the total carotenoid content. The lutein content decreased gradually from a maximum value of 165.03 μg·g^{-1} at S1 to a minimum value of 51.83 μg·g^{-1} at S5. β-Carotene accounted for between 6.31% and 8.57% of total carotenoid content, decreasing from the maximum value (17.33 μg·g^{-1}) at S1 to the minimum value (4.62 μg·g^{-1}) at S5. The contents of other carotenoid metabolites were relatively low, of which α-carotene decreased-increased-decreased; zeaxanthin and β-cryptoxanthin increased-decreased-increased; (E/Z)-phytoene, capsorubin, and violaxanthin dibutyrate increased-decreased; neoxanthin and lutein dilaurate decreased-increased; and violaxanthin and neochrome palmitate decreased and increased, respectively. With the exception of violaxanthin, the trends exhibited by the other carotenoids and total carotenoids were inconsistent, and their contents were minimal, not constituting the primary carotenoid components.

In summary, lutein is the main carotenoid involved in peel coloration, and changes in its content are the main cause of changes in the total carotenoid content. The decline in lutein content resulted in a gradual weakening of the yellowing effect of carotenoids in the process of fruit color change in 'Zizhenzhu'.

Analysis of chlorophyll metabolites in peel during fruit development. As shown in Fig. 8, with the development of 'Zizhenzhu' hawthorn fruits, the total chlorophyll content of the peel decreased from a maximum value of 297.99 μg·g^{-1} at S1 to a minimum value of 73.68 μg·g^{-1} at S5. The chlorophyll a content was slightly higher than that of chlorophyll b, but the contents of both changed in the same manner. Therefore, chlorophyll is the main factor in the green color of hawthorn peel at the early stage of fruit development; as the chlorophyll content decreases, the green color of the peel gradually weakens.

Analysis of peel-coloration metabolites during fruit development. Correlation analysis of 'Zizhenzhu' peel-coloration metabolites and peel color difference values indicated that anthocyanins were significantly positively correlated with the a* value of peel ($r = 0.939$, $P < 0.01$), whereas chlorophyll was

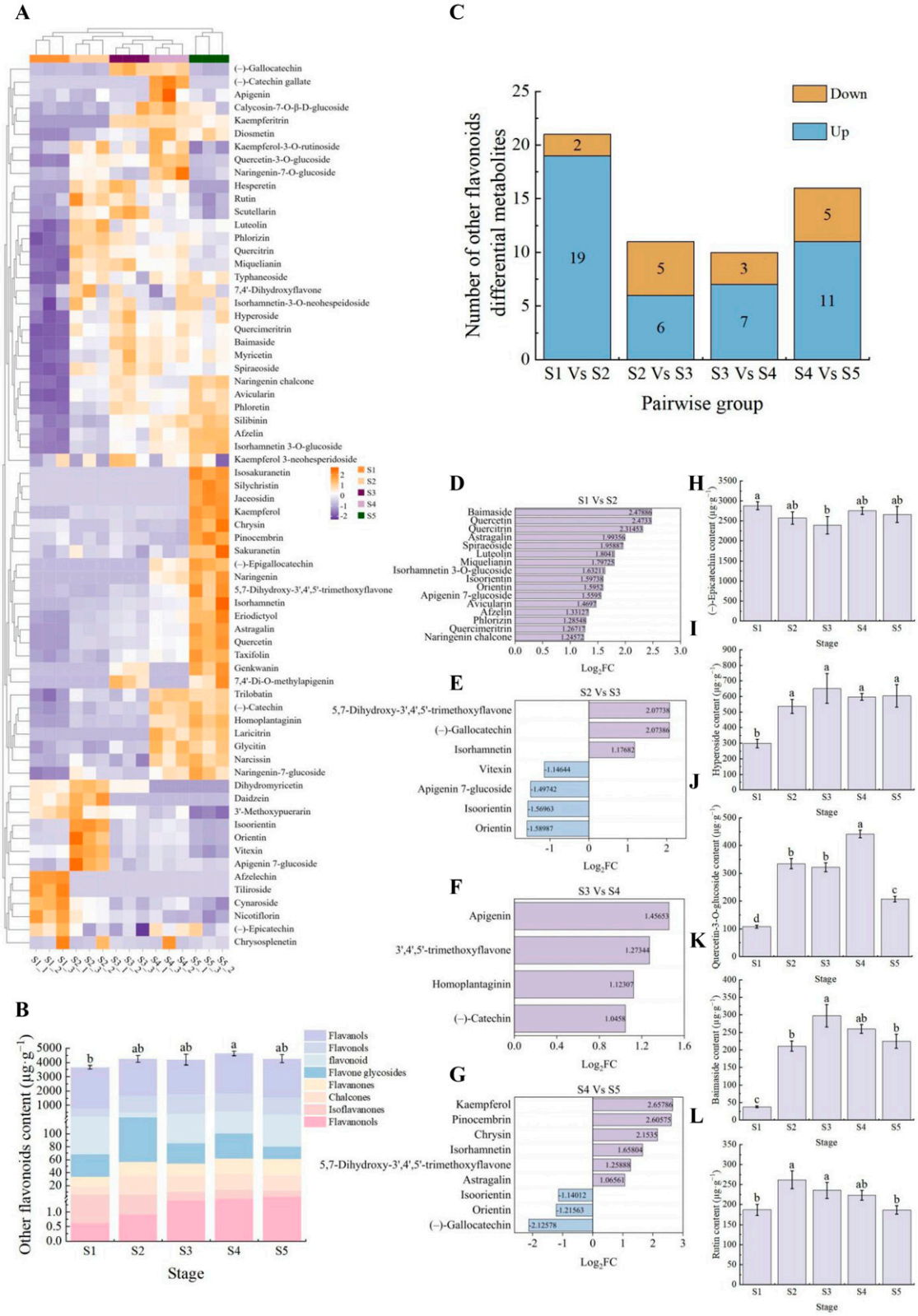

Fig. 5. Analysis of other flavonoid metabolites in the peel during 'Zizhenzhu' fruit development. (**A**) Heatmap of other flavonoid metabolites clustering in the peel of 'Zizhenzhu' during fruit development. Each column in the heatmap represents a sample and each row represents a metabolite. Different colors in the heatmap represent different metabolite contents. Yellow and purple colors indicate higher or lower metabolite levels, respectively. (**B**) Changes in the content of other flavonoid components in the 'Zizhenzhu' peel. (**C**) The number of upregulated and downregulated differential other flavonoid metabolites in the 'Zizhenzhu' peel. (**D–G**) Histograms of the differential multiplicity of other flavonoid differential metabolites in the 'Zizhenzhu' peel ($Log_2FC \neq \pm Inf$). (**H**) Changes in the content of (–)-epicatechin in the 'Zizhenzhu' peel. (**I**) Changes in the content of hyperoside in the 'Zizhenzhu' peel. (**J**) Changes in the content of quercetin-3-O-glucoside in the 'Zizhenzhu' peel. (**K**) Changes in the content of baimaside in the 'Zizhenzhu' peel. (**L**) Changes in the content of rutin in the 'Zizhenzhu' peel. Values of three replicates are expressed as the mean ± standard deviation and different letters indicate significant differences between groups ($P < 0.05$).

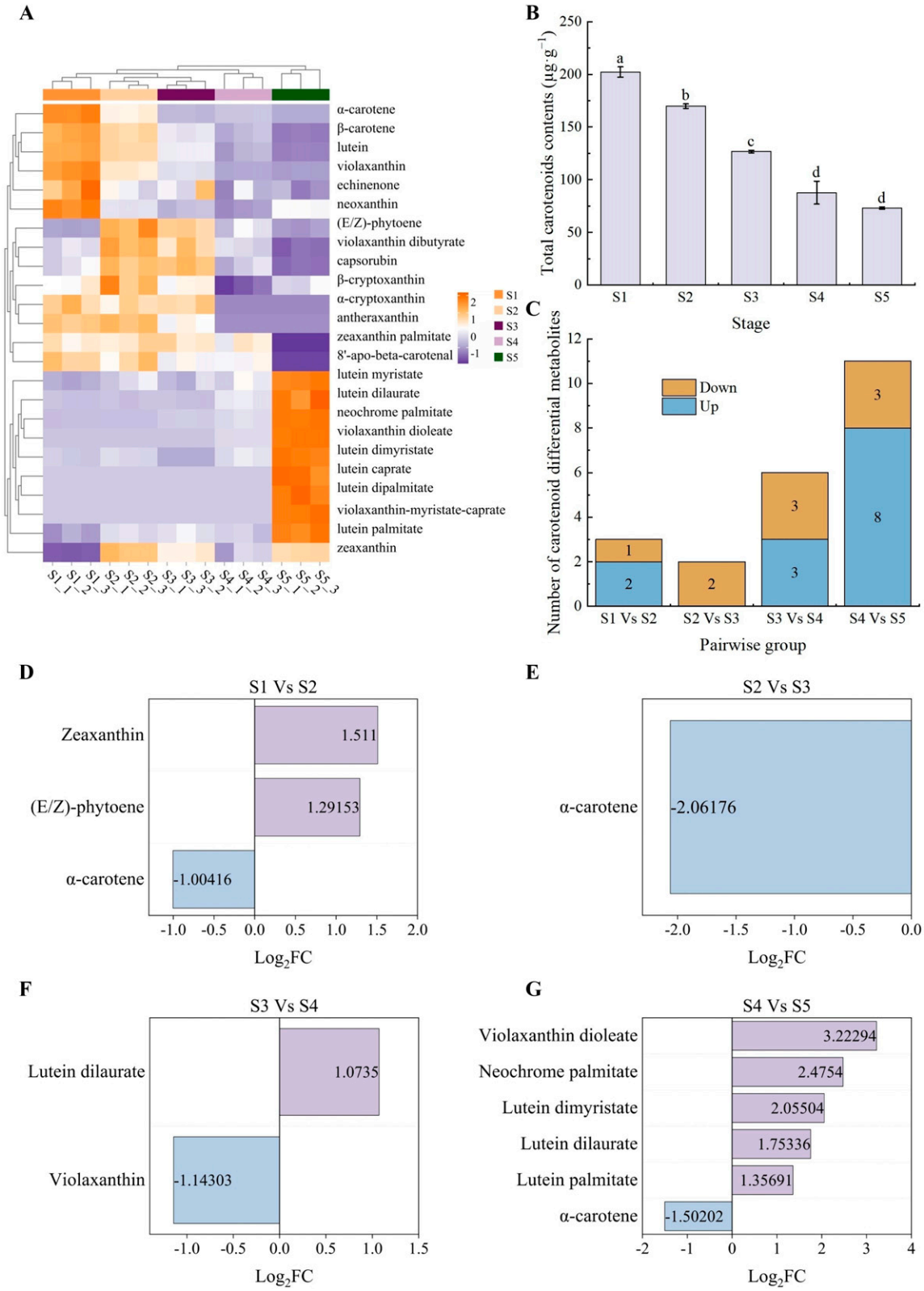

Fig. 6. Analysis of carotenoid metabolites in the peel during 'Zizhenzhu' fruit development. (**A**) Heatmap of carotenoid metabolites clustering in the peel of 'Zizhenzhu' during fruit development. Each column in the heatmap represents a sample and each row represents a metabolite. Different colors in the heatmap represent different metabolite contents. Yellow and purple colors indicate higher or lower metabolite levels, respectively. (**B**) Changes in the content of total carotenoids in the 'Zizhenzhu' peel. (**C**) The number of upregulated and downregulated differential carotenoid metabolites in the 'Zizhenzhu' peel. (**D–G**) Histograms of the differential multiplicity of carotenoid differential metabolites in 'Zizhenzhu' peel ($Log_2FC \neq \pm Inf$).

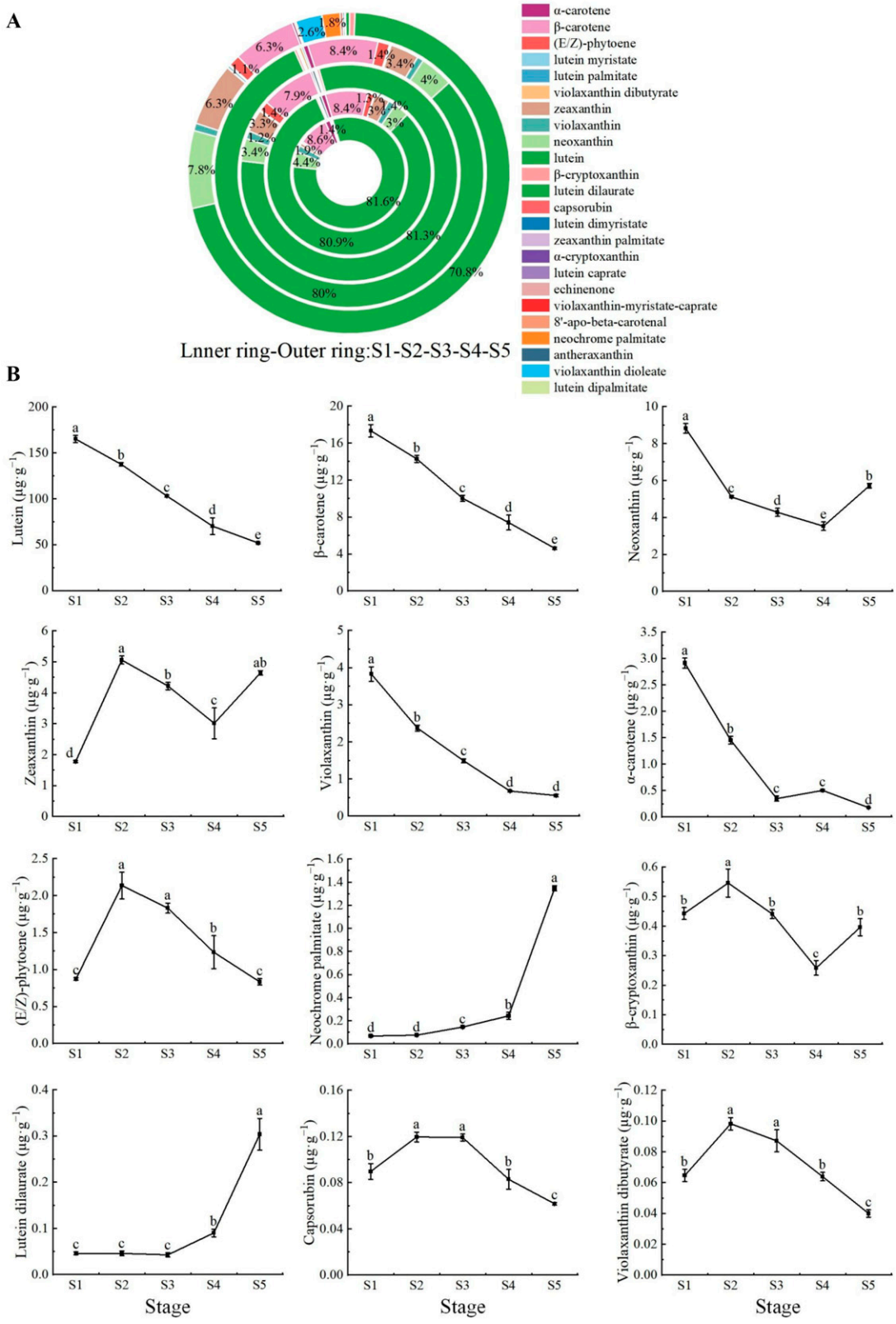

Fig. 7. Analysis of carotenoid components in the peel during 'Zizhenzhu' fruit development. (**A**) The percentage of carotenoid content in the five periods of 'Zizhenzhu' (inner ring to outer ring is five developmental periods S1-S2-S3-S4-S5). (**B**) Changes in the content of 12 major carotenoid components during the five periods of 'Zizhenzhu'. Values of three replicates are expressed as the mean ± standard deviation and different letters indicate significant differences between groups ($P < 0.05$).

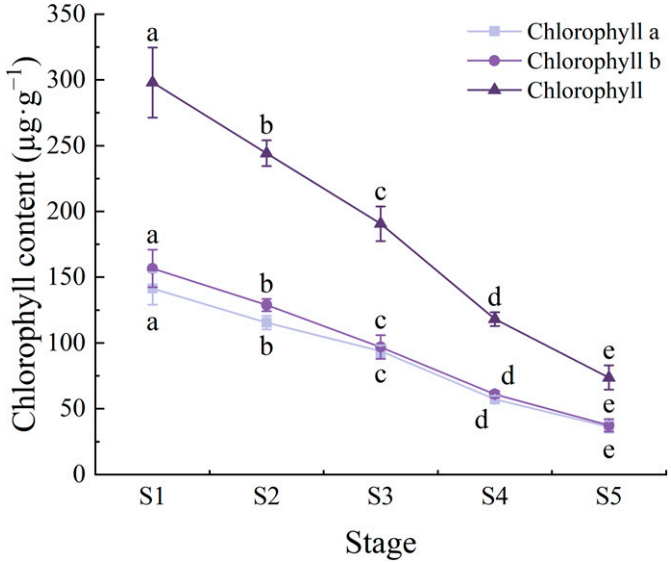

Fig. 8. Changes in the content of chlorophyll in the 'Zizhenzhu' peel. Values of three replicates are expressed as the mean ± standard deviation. Different letters indicate significant differences between groups ($P < 0.05$).

significant negatively correlated with the a* value of peel ($r = -0.925$, $P < 0.01$); carotenoids were significantly positively correlated with the b* value of peel ($r = 0.932$, $P < 0.01$), whereas the correlation of the other flavonoids with the b* value was not significant ($r = -0.486$, $P > 0.05$), indicating that there was little correlation between the other flavonoids and fruit color.

To further elucidate the metabolite mechanism underlying the color change in 'Zizhenzhu' hawthorn fruit, a correlation analysis of anthocyanins, carotenoids, and chlorophyll was conducted. As shown in Fig. 9, the anthocyanin content increased, while the carotenoid and chlorophyll contents decreased in conjunction with fruit development. The anthocyanin content gradually increased from a value of 20.09 μg·g^{-1} at S1 to a value of 1724.69 μg·g^{-1} at S5. The carotenoid content was the maximum value (202.26 μg·g^{-1}) at S1 and was 10.07 times higher than the anthocyanin content at S1; the carotenoid content decreased to the minimum value (73.16 μg·g^{-1}) at S5, when the anthocyanin content was 23.57 times higher than the carotenoid content. The chlorophyll content was the maximum value (297.99 μg·g^{-1}) at S1, which was 14.83 times higher than the anthocyanin content. The chlorophyll content decreased to 73.68 μg·g^{-1} at S5, at which time the content of anthocyanin was 23.41 times higher than that of chlorophyll. In summary, the accumulation of anthocyanin and decrease in carotenoid and chlorophyll were the main reasons for the change of 'Zizhenzhu' fruit color from green to purple.

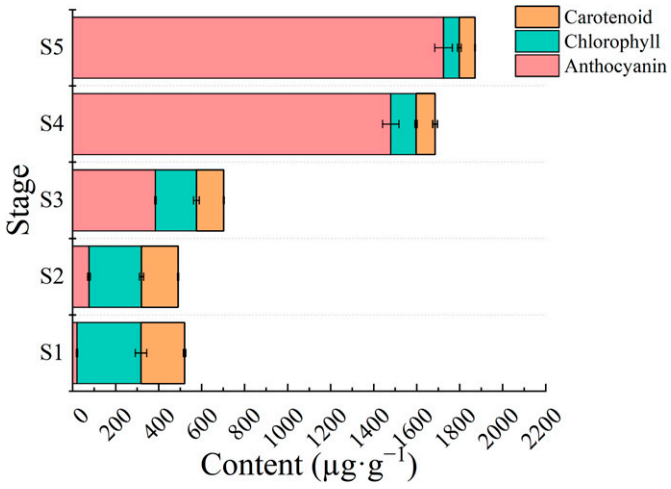

Fig. 9. Correlation analysis between anthocyanin, chlorophyll, and carotenoid metabolites. Values of three replicates are expressed as the mean ± standard deviation.

Discussion

This study used targeted metabolomics (LC-MS/MS) to reveal the peel-coloration metabolite contents of the purple hawthorn 'Zizhenzhu' during the process of coloration. In total, 135 metabolites were detected, including 35 anthocyanins, 6 proanthocyanidins, 68 other flavonoids, 24 carotenoids, and 2 chlorophylls.

The anthocyanin content was significantly positively correlated with 'Zizhenzhu' peel color and followed the same trend as the a* value. This implies that anthocyanin is the key metabolite responsible for the purple coloration of 'Zizhenzhu' during ripening. Anthocyanins cause red, blue, and purple colors in a variety of plants, and the predominant anthocyanin in most plants is cyanidin-3-glucoside (Khoo et al. 2017). Cyanidin derivatives are the main anthocyanins in the four hawthorn varieties: 'DJX', 'DMQ', 'WLH', and 'WLZR' (Yang et al. 2022). Our findings are in accord with recent findings indicating that anthocyanin accumulation, predominantly cyanidin-3-O-galactoside, increases markedly throughout development and is positively correlated with fruit coloration. Therefore, we conclude that cyanidin-3-O-galactoside is the predominant anthocyanin causing 'Zizhenzhu' peel color. 'Zizhenzhu' peel is rich in cyanidin-3-O-galactoside, which is an important anthocyanin derivative with multiple biological significance. In addition to its antioxidant efficacy and immunomodulatory properties, it also affects plant adaptability and ornamental value (Bushmeleva et al. 2022; Li et al. 2023; Lim et al. 2023). The red peel and flesh of a full red-type kiwifruit (*Actinidia arguta*) is closely related to the enrichment of cyanidin-3-O-galactoside (Ye et al. 2023), whereas *Malus spectabilis* leaves show a red phenotype by accumulating cyanidin-3-O-galactoside under drought stress (Xu et al. 2025). This anthocyanin coloration enhances the ornamental value while attracting pollinators, and also enhances plant resistance under abiotic stress (Landi et al. 2021; Zong et al. 2025). Therefore, hawthorn breeding can focus on analyzing the regulatory network of cyanidin-3-O-galactoside synthesis or stabilizing or enhancing the purple phenotype through hybridization to enhance market competitiveness and expand the pharmaceutical application scenarios by combining functional components.

Moreover, the anthocyanin content of 'Ruanzi' hawthorn peels was 930.04 μg·g^{-1} at S5; in comparison, the anthocyanin content of peel in 'Zizhenzhu' was 1.85 times higher under the same growing conditions (Guo et al. 2024). This significant difference implies that the substantial accumulation of anthocyanins caused the peel phenotype to appear purple rather than red. In this study, the significant difference in anthocyanin content of different varieties under the same growth condition resulted in phenotype differences. The differential gene expression level and gene structure should influence the plant phenotype (Xue et al. 2023). Therefore, we will follow-up to further explore the mechanisms of hawthorn

fruit color regulation in 'Zizhenzhu' and other varieties at the gene expression levels or gene structures.

Carotenoids are important coloration metabolites in fruits, and their accumulation and degradation influence peel color (Keawmanee et al. 2022; Tian et al. 2024). Guo et al. (2024) confirmed that during the maturation of 'Jinruyi' and 'Ruanzi' hawthorn, the carotenoid content initially decreased and then increased. In blueberry (*Vaccinium corymbosum*), the carotenoid content initially increased but then decreased due to enhanced metabolism, so the carotenoids did not alter the anthocyanin-dominated fruit color to a yellow or orange phenotype (Li et al. 2024). Our findings are consistent with studies in blueberry, the carotenoid content of 'Zizhenzhu' decreased steadily during ripening, and the anthocyanin content was 23.57 times higher than the carotenoids content at S5. Although carotenoids were positively correlated with the b* value of peel, their low levels would not significantly affect the purple coloration driven by the substantial anthocyanin accumulation.

Furthermore, chlorophyll degradation substantially influences changes in peel color during fruit development. As grapes (*Vitis vinifera*) mature, the chlorophyll content declines, causing the green color to weaken, and the substantial anthocyanin accumulation contributes to the transformation of the fruit color from green to purple (Lu et al. 2022). In wax gourd (*Benincasa hispida*), the chlorophyll content determines the color of the fruit peel, with higher levels resulting in a green hue and lower levels leading to a black appearance (Nong et al. 2023). In our study, the chlorophyll a and b and total chlorophyll contents decreased in the peel of 'Zizhenzhu' fruit during development, which is consistent with previous studies. Initially, the chlorophyll content was 14.83 times higher than the anthocyanin content, whereas in the late stage, the anthocyanin content was 23.41 times higher than the chlorophyll content. This implies that the significantly higher chlorophyll content compared with that of anthocyanin caused the initial green phenotype of 'Zizhenzhu' fruit, whereas the final purple phenotype was due to the significantly higher anthocyanin content compared with that of chlorophyll.

The proanthocyanidin content of 'Zizhenzhu' peel remained consistently high throughout fruit development, implying that proanthocyanidins have relatively little effect on peel color. The high levels may be related to the antioxidant properties of hawthorn (Šamec and Piljac-Žegarac 2011). Furthermore, analysis of additional flavonoids revealed that (–)-epicatechin was the predominant flavonoid, followed by hyperoside. This aligns with previous reports of the yellow appearance of non-anthocyanin flavonoids (Sinopoli et al. 2019). However, our correlation analysis revealed no significant correlation between these flavonoids and the b* value of 'Zizhenzhu' ($r = -0.486$, $P > 0.05$), indicating that they are not the primary coloring substances.

In summary, changes in the ratios of anthocyanin, chlorophyll, and carotenoid content during the development of 'Zizhenzhu' hawthorn affect fruit coloration (Fig. 10). Cyanidin-3-O-galactoside was the pivotal substance for the color of purple hawthorn 'Zizhenzhu' fruit. The decrease in carotenoid and chlorophyll contents gradually weakened their effects on color. The other flavonoids were not substantially correlated with peel color, implying their non-involvement in the coloring of the fruit peel. Specifically, the accumulation of cyanidin-3-O-galactoside-based anthocyanins, in conjunction with the decrease in carotenoid and chlorophyll contents during development, contributed to the change in fruit color from green to purple. Notably, the cyanidin-3-O-galactoside content is significantly higher in 'Zizhenzhu' than in other hawthorn varieties, resulting in the rare purple color instead of the more prevalent red. The study offers insights into the pigmentation mechanism of the purple hawthorn fruit, facilitating further research and breeding efforts in this area.

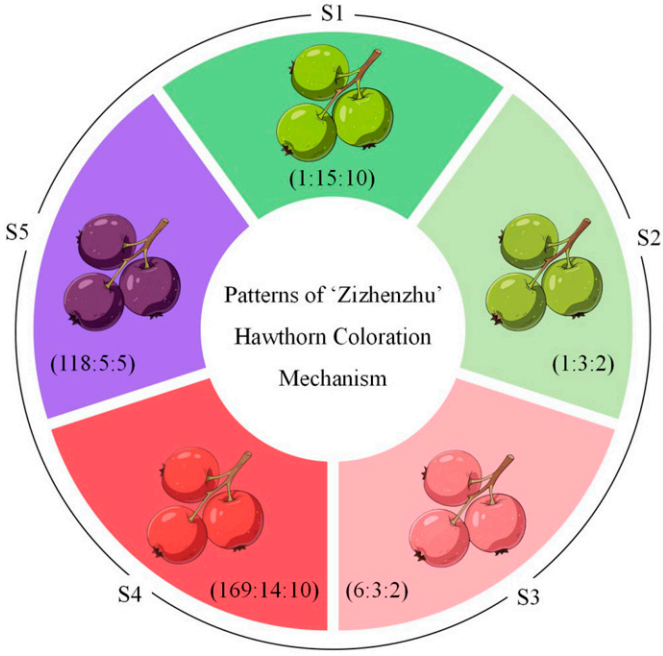

Fig. 10. Patterns of 'Zizhenzhu' hawthorn coloration mechanism. Anthocyanin content: chlorophyll content: carotenoid content is used to represent the color formation mechanism of these three types of coloration metabolites in hawthorn fruits at each developmental stage, for example, the anthocyanin: chlorophyll:carotenoid content of S1 in 'Zizhenzhu' is 1:15:10.

References Cited

Acevedo De la Cruz A, Hilbert G, Rivière C, Mengin V, Ollat N, Bordenave L, Decroocq S, Delaunay J-C, Delrot S, Mérillon J-M, Monti J-P, Gomès E, Richard T. 2012. Anthocyanin identification and composition of wild *Vitis* spp. accessions by using LC-MS and LC-NMR. Anal Chim Acta. 732:145–152. https://doi.org/10.1016/j.aca.2011.11.060.

Amorim-Carrilho KT, Cepeda A, Fente C, Regal P. 2014. Review of methods for analysis of carotenoids. TrAC Trends in Analytical Chemistry. 56:49–73. https://doi.org/10.1016/j.trac.2013.12.011.

Bushmeleva K, Vyshtakalyuk A, Terenzhev D, Belov T, Nikitin E, Zobov V. 2022. Antioxidative and immunomodulating properties of *Aronia melanocarpa* extract rich in anthocyanins. Plants. 11(23). https://doi.org/10.3390/plants11233333.

Cao S, Liang M, Shi L, Shao J, Song C, Bian K, Chen W, Yang Z. 2017. Accumulation of carotenoids and expression of carotenogenic genes in peach fruit. Food Chem. 214:137–146. https://doi.org/10.1016/j.foodchem.2016.07.085.

Çiftci G, Çelebi İ, Ümit F. 2024. Assessment of phenolic, flavonoid, total antioxidant, and anthocyanin contents of various colored hawthorn fruits for their potential as functional foods. Chem Pap. 79(1):575–581. https://doi.org/10.1007/s11696-024-03850-3.

Dai J, Xu Z, Fang Z, Zheng X, Cao L, Kang T, Xu Y, Zhang X, Zhan Q, Wang H, Hu Y, Zhao C. 2024. NAC transcription factor PpNAP4 promotes chlorophyll degradation and anthocyanin synthesis in the

skin of peach Fruit. J Agric Food Chem. 72(36):19826–19837. https://doi.org/10.1021/acs.jafc.4c03924.
Geyer R, Peacock AD, White DC, Lytle C, Van Berkel GJ. 2004. Atmospheric pressure chemical ionization and atmospheric pressure photoionization for simultaneous mass spectrometric analysis of microbial respiratory ubiquinones and menaquinones. J Mass Spectrom. 39(8):922–929. https://doi.org/10.1002/jms.670.
Guo K, Dong G, Nong L, Wang H, Teng C, Meng X. 2024. Targeted metabolomics-based analysis of peel color differences between yellow and red hawthorn. Sci Agric Sin. 57(12):2439–2453. https://doi.org/10.3864/j.issn.0578-1752.2024.12.013.
Hermanns AS, Zhou X, Xu Q, Tadmor Y, Li L. 2020. Carotenoid pigment accumulation in horticultural plants. Hortic Plant J. 6(6): 343–360. https://doi.org/10.1016/j.hpj.2020.10.002.
Huang H, Gao X, Gao X, Zhang S, Zheng Y, Zhang N, Hong B, Zhao X, Gu Z. 2022. Flower color mutation, pink to orange, through CmGATA4-CCD4a-5 module regulates carotenoids degradation in chrysanthemum. Plant Sci. 322:111290. https://doi.org/10.1016/j.plantsci.2022.111290.
Jeknic Z, Morre JT, Jeknic S, Jevremovic S, Subotic A, Chen TH. 2012. Cloning and functional characterization of a gene for capsanthin-capsorubin synthase from tiger lily (*Lilium lancifolium* Thunb. 'Splendens'). Plant Cell Physiol. 53(11):1899–1912. https://doi.org/10.1093/pcp/pcs128.
Jia D, Li Y, Jia K, Huang B, Dang Q, Wang H, Wang X, Li C, Zhang Y, Nie J, Yuan Y. 2024. Abscisic acid activates transcription factor module MdABI5-MdMYBS1 during carotenoid-derived apple fruit coloration. Plant Physiol. 195(3):2053–2072. https://doi.org/10.1093/plphys/kiae188.
Jiang L, Yue M, Liu Y, Ye Y, Zhang Y, Lin Y, Wang X, Chen Q, Tang H. 2022. Alterations of phenylpropanoid biosynthesis lead to the natural formation of pinkish-skinned and white-fleshed strawberry (*Fragaria* × *ananassa*). Int J Mol Sci. 23(13) https://doi.org/10.3390/ijms23137375.
Ji X, Ren J, Lang S, Wang D, Zhu L, Song X. 2020. Differential regulation of anthocyanins in *Cerasus humilis* fruit color revealed by combined transcriptome and metabolome analysis. Forests. 11(10):1065. https://doi.org/10.3390/f11101065.
Keawmanee N, Ma G, Zhang L, Yahata M, Murakami K, Yamamoto M, Kojima N, Kato M. 2022. Exogenous gibberellin induced regreening through the regulation of chlorophyll and carotenoid metabolism in Valencia oranges. Plant Physiol Biochem. 173:14–24. https://doi.org/10.1016/j.plaphy.2022.01.021.
Khoo HE, Azlan A, Tang ST, Lim SM. 2017. Anthocyanidins and anthocyanins: Colored pigments as food, pharmaceutical ingredients, and the potential health benefits. Food Nutr Res. 61(1):1361779. https://doi.org/10.1080/16546628.2017.1361779.
Krinsky NI, Mayne ST, Sies H (eds). 2004. Carotenoids in health and disease (1st ed.). CRC Press, Boca Raton, FL, USA. https://doi.org/10.1201/9780203026649.
Landi M, Agati G, Fini A, Guidi L, Sebastiani F, Tattini M. 2021. Unveiling the shade nature of cyanic leaves: A view from the ''blue absorbing side'' of anthocyanins. Plant Cell Environ. 44(4):1119–1129. https://doi.org/10.1111/pce.13818.
Li J, Shi C, Shen D, Han T, Wu W, Lyu L, Li W. 2022. Composition and antioxidant activity of anthocyanins and non-anthocyanin flavonoids in blackberry from different growth stages. Foods. 11(18):2902. https://doi.org/10.3390/foods11182902.
Li X, Zhang D, Pan X, Kakar KU, Nawaz Z. 2024. Regulation of carotenoid metabolism and ABA biosynthesis during blueberry fruit ripening. Plant Physiol Biochem. 206:108232. https://doi.org/10.1016/j.plaphy.2023.108232.
Li Y, Sun Z, Lu J, Jin Z, Li J. 2023. Integrated transcriptomics and metabolomics analysis provide insight into anthocyanin biosynthesis for sepal color formation in *Heptacodium miconioides*. Front Plant Sci. 14:1044581. https://doi.org/10.3389/fpls.2023.1044581.
Li Y, Li T, Yan Z, Bariami W, Wu C, Yan S, Fan G, Li X, Zhou D, Cong K, Cheng J. 2024. Carotenoids in berries: Composition, benefits, metabolic processes and influencing factors - A review. Sci Hortic. 329:112956. https://doi.org/10.1016/j.scienta.2024.112956.
Lim YJ, Park H, Kim W, Eom SH. 2023. Ultraviolet B-induced increase of cyanidin-3-O-galactoside, quercetin-3-O-galactoside, and ursolic acid enhances antioxidant and anti-inflammatory activities in apples. Postharvest Biol Technol. 206:112580. https://doi.org/10.1016/j.postharvbio.2023.112580.
Liu S, Zhang Y. 2024. Antioxidant properties and electrochemical activity of anthocyanins and anthocyanidins in mulberries. Food Measure. 18(5):3569–3576. https://doi.org/10.1007/s11694-024-02426-9.
Liu Q, Wang L, He L, Lu Y, Wang L, Fu S, Luo X, Zhang Y. 2024. Metabolome and transcriptome reveal chlorophyll, carotenoid, and anthocyanin jointly regulate the color formation of *Triadica sebifera*. Physiol Plant. 176(2):e14248. https://doi.org/10.1111/ppl.14248.
Liu Y, Feng X, Zhang Y, Zhou F, Zhu P. 2021. Simultaneous changes in anthocyanin, chlorophyll, and carotenoid contents produce green variegation in pink-leaved ornamental kale. BMC Genomics. 22(1): 455. https://doi.org/10.1186/s12864-021-07785-x.
Lu S, Zhang M, Zhuge Y, Fu W, Ouyang Q, Wang W, Ren Y, Pei D, Fang J. 2022. VvERF17 mediates chlorophyll degradation by transcriptional activation of chlorophyll catabolic genes in grape berry skin. Environ Exp Bot. 193:104678. https://doi.org/10.1016/j.envexpbot.2021.104678.
Muhammad N, Liu Z, Wang L, Yang M, Liu M. 2024. The underlying molecular mechanisms of hormonal regulation of fruit color in fruit-bearing plants. Plant Mol Biol. 114(5):104. https://doi.org/10.1007/s11103-024-01494-1.
Ni X, Ni Z, Ouma KO, Gao Z. 2022. Mutations in PmUFGT3 contribute to color variation of fruit skin in Japanese apricot (*Prunus mume* Sieb. et Zucc.). BMC Plant Biol. 22(1):304. https://doi.org/10.1186/s12870-022-03693-8.
Nong L, Wang P, Yang W, Liu T, Su L, Cheng Z, Bai W, Deng Y, Chen Z, Liu Z. 2023. Analysis of BhAPRR2 allele variation, chlorophyll content, and chloroplast structure of different peel colour varieties of wax gourd (*Benincasa hispida*) and development of molecular markers. Euphytica. 219(10):107. https://doi.org/10.1007/s10681-023-03233-x.
Qin Y, Hao X, Li Q, Wang Y, Dong G. 2022. Diversity analysis of phenotypic characters in germplasm resources of hawthorn. Journal of Fruit Science. 39(10):1759–1773. https://doi.org/10.13925/j.cnki.gsxb.20220102.
Šamec D, Piljac-Žegarac J. 2011. Postharvest stability of antioxidant compounds in hawthorn and cornelian cherries at room and refrigerator temperatures—Comparison with blackberries, white and red grapes. Sci Hortic. 131:15–21. https://doi.org/10.1016/j.scienta.2011.09.021.
Schweiggert RM, Vargas E, Conrad J, Hempel J, Gras CC, Ziegler JU, Mayer A, Jimenez V, Esquivel P, Carle R. 2016. Carotenoids, carotenoid esters, and anthocyanins of yellow-, orange-, and red-peeled cashew apples (*Anacardium occidentale* L.). Food Chem. 200:274–282. https://doi.org/10.1016/j.foodchem.2016.01.038.
Sharma H, Sharma P, Kumar A, Chawla N, Dhatt AS. 2024. Multifaceted regulation of anthocyanin biosynthesis in plants: A comprehensive review. J Plant Growth Regul. 43(9):3048–3062. https://doi.org/10.1007/s00344-024-11306-x.
Shi B, Chen N, Li F, Yuan F, Yan L, Wang J, Li P. 2023. Flavonoid content and developmental changes in passion fruit. (*Passiflora edulis*). South China Fruits. 52(01):97–100. https://doi.org/10.13938/j.issn.1007-1431.20220139.
Sinopoli A, Calogero G, Bartolotta A. 2019. Computational aspects of anthocyanidins and anthocyanins: A review. Food Chem. 297:124898. https://doi.org/10.1016/j.foodchem.2019.05.172.
Song H, Lu Q, Song T, Gao C, Zhu W, Guo X. 2024. Study on the mechanism of carotenoid production and accumulation in orange red

carrot (*Daucus carota* L.). Sci Hortic. 327:112825. https://doi.org/10.1016/j.scienta.2023.112825.
Tian S, Yang Y, Fang B, Uddin S, Liu X. 2024. The CrMYB33 transcription factor positively coordinates the regulation of both carotenoid accumulation and chlorophyll degradation in the peel of citrus fruit. Plant Physiol Biochem. 209:108540. https://doi.org/10.1016/j.plaphy.2024.108540.
Wang X, Yang C, Zhu W, Weng Z, Li F, Teng Y, Zhou K, Qian M, Deng Q. 2024. Transcriptomic analysis reveals the mechanism of color formation in the peel of an evergreen pomegranate cultivar 'Danruo No.1' during fruit development. Plants (Basel). 13(20):2903. https://doi.org/10.3390/plants13202903.
Wang Y, Hao R, Guo R, Nong H, Qin Y, Dong N. 2023. Integrative analysis of metabolome and transcriptome reveals molecular insight into metabolomic variations during hawthorn fruit development. Metabolites. 13(3):423. https://doi.org/10.3390/metabo13030423.
Wang Y, Zhang C, Dong B, Fu J, Hu S, Zhao H. 2018. Carotenoid accumulation and its contribution to flower coloration of *Osmanthus fragrans*. Front Plant Sci. 9:1499. https://doi.org/10.3389/fpls.2018.01499.
Wei J, Mu X, Wang S, Wei Q, Zhu L, Zhang X, Zhang J, Liu X, Wen B, Li M, Liu J. 2025. Integrated metabolome and transcriptome analysis provides insights into the mechanisms of terpenoid biosynthesis in tea plants (*Camellia sinensis*). Food Res Int. 201:115542. https://doi.org/10.1016/j.foodres.2024.115542.
Xu Y, Liu Y, Yue L, Zhang S, Wei J, Zhang Y, Huang Y, Zhao R, Zou W, Feng H, Li H. 2025. MsERF17 promotes ethylene-induced anthocyanin biosynthesis under drought conditions in *Malus spectabilis* leaves. Plant Cell Environ. 48(3):1890–1902. https://doi.org/10.1111/pce.15271.
Xue C, Qiu F, Wang Y, Li B, Zhao KT, Chen K, Gao C. 2023. Tuning plant phenotypes by precise, graded downregulation of gene expression. Nat Biotechnol. 41(12):1758–1764. https://doi.org/10.1038/s41587-023-01707-w.
Yang C, Sun N, Qin X, Liu Y, Sui M, Zhang Y, Hu Y, Mao Y, Shen X. 2024. Analysis of flavonoid metabolism of compounds in succulent fruits and leaves of three different colors of Rosaceae. Sci Rep. 14(1):4933. https://doi.org/10.1038/s41598-024-55541-4.
Yang C, Wang X, Zhang J, Li N, Wu R, Wang T, Ding W. 2022. Comparative metabolomic analysis of different-colored hawthorn berries (*Crataegus pinnatifida*) provides a new interpretation of color trait and antioxidant activity. LWT. 163:113623. https://doi.org/10.1016/j.lwt.2022.113623.
Ye L, Bai F, Zhang L, Luo M, Gao L, Wang Z, Peng J, Chen Q, Luo X. 2023. Transcriptome and metabolome analyses of anthocyanin biosynthesis in post-harvest fruits of a full red-type kiwifruit (*Actinidia arguta*) 'Jinhongguan'. Front Plant Sci. 14:1280970. https://doi.org/10.3389/fpls.2023.1280970.
Yu Z, Liao Y, Teixeira da Silva JA, Yang Z, Duan J. 2018. Differential accumulation of anthocyanins in *Dendrobium officinale* stems with red and green peels. Int J Mol Sci. 19(10):2857. https://doi.org/10.3390/ijms19102857.
Yuan X, Sun W, Zou X, Liu B, Huang W, Chen Z, Li Y, Qiu MY, Liu ZJ, Mao Y, Zou SQ. 2018. Sequencing of *Euscaphis konishii* endocarp transcriptome points to molecular mechanisms of endocarp coloration. Int J Mol Sci. 19(10):3209. https://doi.org/10.3390/ijms19103209.
Zan W, Wu Q, Dou S, Wang Y, Zhu Z, Xing S, Yu Y. 2024. Analysis of flower color diversity revealed the co-regulation of cyanidin and peonidin in the red petals coloration of *Rosa rugosa*. Plant Physiol Biochem. 216:109126. https://doi.org/10.1016/j.plaphy.2024.109126.
Zhang A, Yang H, Ji S, Tian C, Chen N, Gong H, Li J. 2022. Metabolome and transcriptome analyses of anthocyanin accumulation mechanisms reveal metabolite variations and key candidate genes involved in the pigmentation of *Prunus tomentosa* Thunb. cherry fruit. Front Plant Sci. 13:938908. https://doi.org/10.3389/fpls.2022.938908.
Zhang J, Chai X, Zhao F, Hou G, Meng Q. 2022. Food applications and potential health benefits of hawthorn. Foods. 11(18):2861. https://doi.org/10.3390/foods11182861.
Zhang S, Li T, Liu S, Qi X, Yang Y, Zhang J, Jia L, Wang P, Mu X. 2025. Integrated transcriptomics and metabolomics reveal key genes and metabolic pathway in flower and fruit color formation of *Cerasus humilis* (Bge.) Sok. Plants (Basel). 14(7):1103. https://doi.org/10.3390/plants14071103.
Zhao X, Feng Y, Ke D, Teng Y, Yuan Z. 2024. Comparative transcriptomic and metabolomic profiles reveal fruit peel color variation in two red pomegranate cultivars. Plant Mol Biol. 114(3):51. https://doi.org/10.1007/s11103-024-01446-9.
Zhao Y, Li A, Qi S, Su K, Guo Y. 2022. Identification of candidate genes related to anthocyanin biosynthesis in red sarcocarp hawthorn (*Crataegus pinnatifida*). Sci Hortic. 298:110987. https://doi.org/10.1016/j.scienta.2022.110987.
Zhao Z, Adjei MO, Luo R, Yu H, Pang Y, Wang J, Zhang Y, Ma J, Gao A. 2024. Metabolome and transcriptome analysis reveal the pigments biosynthesis pathways in different color fruit peels of *Clausena lansium* L. Skeels. Front Plant Sci. 15:1496504. https://doi.org/10.3389/fpls.2024.1496504.
Zhu F, Luo T, Liu C, Wang Y, Yang H, Yang W, Zheng L, Xiao X, Zhang M, Xu R, Xu J, Zeng Y, Xu J, Xu Q, Guo W, Larkin RM, Deng X, Cheng Y. 2017. An R2R3-MYB transcription factor represses the transformation of alpha- and beta-branch carotenoids by negatively regulating expression of CrBCH2 and CrNCED5 in flavedo of *Citrus reticulate*. New Phytol. 216(1):178–192. https://doi.org/10.1111/nph.14684.
Zhu K, Zeng Y, Lin H, Tang Y, He Y, Zheng S, Chen Y. 2024. Variability in leaf color induced by chlorophyll deficiency: Transcriptional changes in bamboo leaves. Curr Issues Mol Biol. 46(2):1503–1515. https://doi.org/10.3390/cimb46020097.
Zhuang B, Li H, Shu C, Pu T, Wang J, Wang T, Wang Z. 2023. The classification, molecular structure and biological biosynthesis of flavonoids, and their roles in biotic and abiotic stresses. Molecules. 28(8):3599. https://doi.org/10.3390/molecules28083599.
Zong Y, Zhao Z, Zhou K, Duan X, Han B, He C, Huang H, Jiang H. 2025. Metabolome and transcriptome analysis of anthocyanin biosynthesis reveal key metabolites and candidate genes in red-stemmed alfalfa (*Medicago sativa*). BMC Genomics. 26(1):323. https://doi.org/10.1186/s12864-025-11529-6.